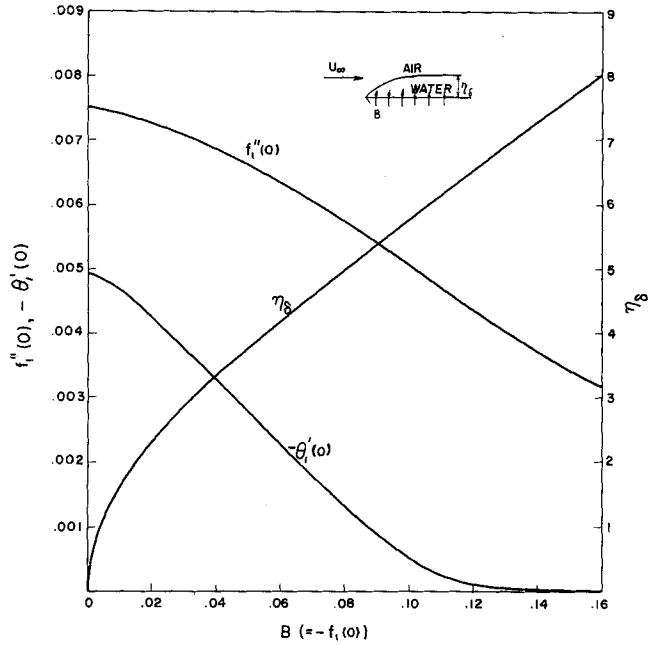

Fig. 2. Effects of the release rate of water into air stream on heat transfer and skin friction.

ing a decrease in both heat transfer and skin friction. The effect will be most severe for the release of air into water stream, for which $(\rho_2\mu_2/\rho_1\mu_1)^{1/2}$ can attain very high values. Therefore the cocurrent flow may be applied as a means to reduce the drag experienced by bodies moving through liquids and transpiration cooling of heated surface.

NOTATION

B = blowing parameter
f = dimensionless stream function defined as $\psi/(U_\infty\nu x)^{1/2}$
k = fluid thermal conductivity
N_{Nu} = Nusselt number
N_{Pr} = Prandtl number
N_{Re} = Reynolds number
T = fluid temperature inside the boundary layer
T_w = wall temperature
T_∞ = free-stream temperature
U_∞ = free-stream velocity
V_1 = blowing velocity at surface, $\frac{B}{2}(U_\infty\nu_1/x)^{1/2}$
x = coordinate along plate
y = coordinate normal to plate

Greek Letters

δ = thickness of inner boundary layer
η = similarity variable, $\eta_1 = 1/2\, y(U_\infty/\nu_1 x)^{1/2}$, $\eta_2 = \frac{y-\delta}{2}(U_\infty/\nu_2 x)^{1/2}$
η_δ = $1/2\,\delta(U_\infty/\nu_1 x)^{1/2}$
θ = $(T-T_\infty)/(T_w-T_\infty)$
μ = absolute viscosity
ν = kinetic viscosity
ρ = fluid density
τ = wall shear stress
ψ = stream function

Subscripts

1 = inner boundary layer (foreign fluid)
2 = outer boundary layer (main stream)

LITERATURE CITED

1. Sparrow, E. M., V. K. Johnson, and E. R. G. Eckert, *J. Appl. Mech.*, Ser. E, **29**, 408-411 (1962).
2. Koh, J. C., *Intern. J. Heat Mass Transfer*, **5**, 941-954 (1962).
3. Cess, R. D., and E. M. Sparrow, *J. Heat Transfer*, C83, 370-376 (1961).
4. *Ibid.*, 377-378.

A Generalized Equation for Solids Distribution in the Semifluidized MT Reactor

K. BABU RAO and L. K. DORAISWAMY

National Chemical Laboratory, Poona, India

A new type of fluid-solid contact operation, called *semifluidization*, was proposed by Fan et al. (*11*), and a few further studies on this technique have also been reported (*6, 10*). Babu Rao et al. (*3*) have utilized the principle of semifluidization for proposing a new type of combined MT reactor system. The MT combination denotes a fully mixed reactor followed by a tubular reactor. The characteristic features of MT reactors have been discussed at length (*1, 9, 14*), and the advantages of using the semifluidized bed for an MT combination have been outlined (*3*). However, the existing information on the mechanics of semifluidization (which is essential in designing an MT semifluidized bed reactor) is fragmentary, and the correlations of Fan and collaborators provide significant guidelines for further work in this area.

The dimensionless relationship proposed (*6, 10*)

$$\left(\frac{h-h_s}{h-h_p}\right) \text{ vs. } \left(\frac{G_s-G_{mf}}{G_t-G_{mf}}\right) \qquad (1)$$

has been derived for a semifluidized bed without the complicating features introduced by the use of a tubular bundle at the top for promoting piston flow. In an MT semifluidized bed reactor the height of the tubular portion will vary, depending on the number of tubes, since the total quantity of solids forming the packed bed below the restraining plate would be the same regardless of the number of tubes at a given semifluidization velocity. Equation (1) cannot therefore be applied to this reactor. Another feature of Equation (1) which needs closer analysis is the assumption that the height of the packed section when all the solids have been conveyed to the

upper portion of the reactor is equal to that of the least static bed.

The object of the present communication is threefold: to verify the correctness of the assumption implicit in Equation (1), to develop a generalized equation for predicting the distribution of solids in an MT semifluidized bed reactor, and to assess the correctness of the generalized equation for predicting the onset of semifluidization (that is, the *minimum* semifluidization velocity).

EXPERIMENTAL STUDIES

The experimental assembly used was essentially similar to that reported earlier (Figure 3 of reference 3) but with provision for solids discharge at the reactor bottom. Two semifluidized columns were used, one of 1.54 in. diam. and the other 4 in. diam. Column 1 was constructed from glass, while column 2 was made of stainless steel. Both these columns could be used either as simple semifluidization columns with perforated restraining plates which could be kept at any height, or as MT reactors with tubular bundles which could also be maintained at any height. The tubular bundle for the glass reactor was composed of five tubes of 0.24 in. diam. and 3 in. high, while that of the larger reactor was composed of nineteen stainless steel tubes of 0.4 in. diam. and 9.5 in. high. Experiments were carried out both with and without the tubular bundles.

In carrying out a run (with a simple restraining plate or a tube bundle), a weighed quantity of solids was placed in the reactor and compressed air was passed through it at the desired velocity. To obtain the exact static bed height at the beginning of a run, the bed was fluidized and resettled several times and the average static height measured. The velocity of the fluid was then increased until the onset of semifluidization as indicated by a sharp rise in the ΔP vs. G curve (see Figure 4 of reference 3). As the velocity is increased beyond the semifluidization point, the height of the packed bed increases until eventually at the terminal velocity the entire bed is in the packed portion.

To measure the distribution of the solids in the packed and fluidized portions for a given velocity (above the minimum semifluidization velocity), the packed portion was allowed to form and the fluidizing portion at the bottom was then removed through the outlet provided, and weighed.

DEVELOPMENT OF GENERALIZED EQUATION

The fluidized bed exists between two extreme limits of velocity: velocity for the onset of fluidization, and the terminal velocity of the solids involved. For the semifluidized bed, on the other hand, the significant velocity is the terminal velocity, and while theoretically the semifluidized bed can exist beyond G_t, it is truly not a semifluidized bed in the absence of the lower fluidizing portion. The minimum fluidization velocity is not significant since the upper packed portion is absent until the onset of semifluidization.

Maximum Semifluidization (Terminal) Velocity

Fan and co-workers (*6, 10*) have suggested three methods of estimating G_t: linear extrapolation of E_f vs. G curves to $E_f = 1$; extrapolation of h_p/h_s vs. G curve to $h_p/h_s = 1$; and use of the equation for free-fall terminal velocity. Normally the correctness or otherwise of the use of these methods for estimating G_t can only be established by measuring the porosity of the packed portion of the semifluidized reactor at different velocities (greater than G_{ms}). For this purpose a suitable porosity measurement device was developed which is briefly described below.

Several methods for determining the porosity of fixed and fluidized beds are available. The most commonly used methods are: measurement of the emitted light by a photocell (*18*), light absorption (*17*), use of a capacitance probe (*7, 8*), acoustic method (*13*), electric charge method (*2*), use of a modified thermister probe

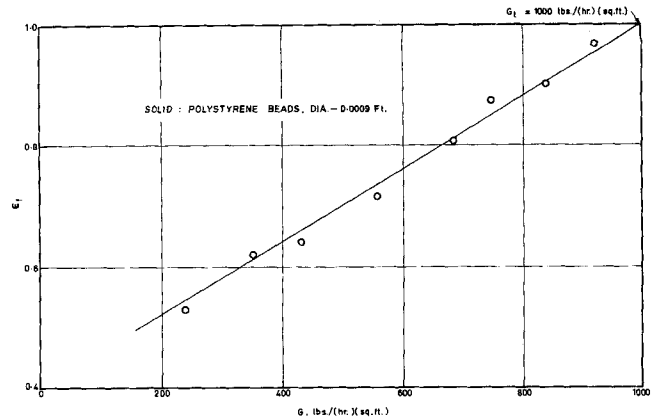

Fig. 1. Determination of G_t from fluidization data.

(*4*), and use of x-rays (*16*). Among these methods it was found that instruments based on capacitance measurement are reliable and relatively simple to make. A technique was therefore devised in which the fluidization column was held between two capacitance plates ½ cm. wide (thus eliminating any disturbances caused by using a probe), and the capacitance of the solids in the section of the column covered by the plates was measured. A calibration curve was prepared for each of the solids used so that the porosity of the packed portion could be read directly from this curve. The correctness of the porosity values measured by this instrument was established by determining the porosities of beds of known voidage.

A typical curve of E_f as a function of G is shown in Figure 1. It can be seen that for the particular solid used, G_t at $E_f = 1$ has a value of 1,000. This method is not considered very accurate since the measurement of the porosity of thinly populated beds is not very accurate. The second method for determining G_t involves the assumption that the height of the packed portion is equal to that of the least static bed. This assumption can be verified by measuring the porosity of the packed bed as a function of velocity. A typical plot is shown in Figure 2, from which it is clear that the ratio E_p/E_s first decreases and then levels off as G_t is approached (as evidenced by the carryover of all the solids to the packed portion). There is a fall in porosity to the extent of 15%. The correct method of measuring G_t by this method would be to determine experimentally the actual value of E_p/E_s for a given solid and then to apply the necessary correction to the value obtained by extrapolating the h_p/h_s vs. G curve to $h_p/h_s = 1$. A typical h_p/h_s vs. G curve is shown in Figure 3. After applying the 15% correction to the value obtained from this figure, the value of G_t works out to 816. But when this correction is not applied the value

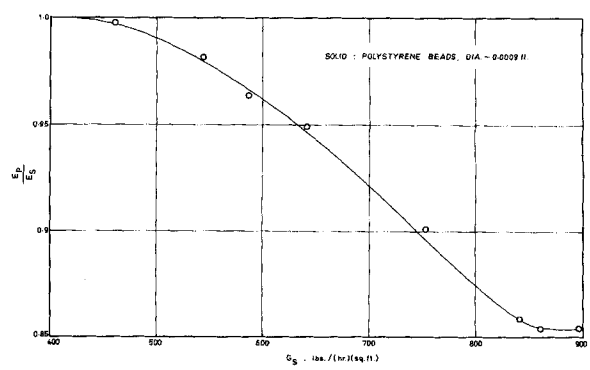

Fig. 2. Effect of semifluidization velocity on the porosity of the packed bed.

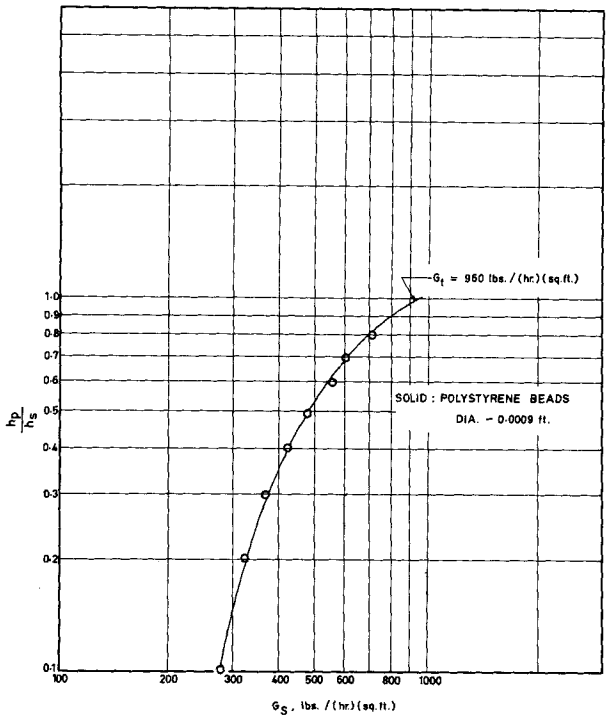

Fig. 3. Determination of G_t from h_p/h_s data.

of G_t is considerably higher (960). This accounts for the consistently higher values of G_t obtained with this method by Fan and co-workers.

The third method of calculating G_t involves the use of the equation

$$G_t = 0.152 \frac{d_p^{1.14}\, g_c^{0.714}\, (\rho_s - \rho_F)^{0.714}}{\mu^{0.428}\, \rho_F^{0.428}} \qquad (2)$$

which is based on Stokes-Einstein equation. G_t calculated by this equation (for the same solid considered for the other two cases) has the value 855. It will thus be seen that the second method, after applying the necessary correction, gives approximately the same value as obtained from Equation (2). This has been found to be true for all the solids included in the present study. Since Equation (2) is general, and the use of the second method involves experimental data, G_t for all the systems in this investigation has been calculated by the third method.

Correlation of Data

As pointed out earlier, G_t is the principal parameter in defining the performance of a semifluidized MT reactor, in addition to the static and semifluidized bed heights and properties of the solids and fluids. The limits of the fluidized bed have generally been expressed in terms of the Archimedes group (*4, 5, 12*). For the semifluidized bed the Archimedes group can be defined as

$$Ar = \frac{d_p^3\, g_c\, \rho_s\, (\rho_s - \rho_F)}{\mu^2} \qquad (3)$$

Since the semifluidization velocity lies between the terminal and minimum semifluidization velocities, the Archimedes group logically can be expected to account for the viscous and gravitational forces in the bed. In addition, the semifluidization characteristics have to be defined by a separate group, which would account for the distribution of solids between the packed and fluidized portions and also the heights of the static and semifluidized beds. Such a group can be defined as

$$Sf = \frac{(W_s - W_p)}{(h - h_s)^3\, \rho_s} \qquad (4)$$

For a reactor of given diameter, the performance of a semifluidized MT reactor can therefore be expressed as

$$\frac{G_s}{G_t} = k\, (Ar)^a\, (Sf)^b \qquad (5)$$

where G_s/G_t represents the ratio of the semifluidization velocity to the terminal velocity. This equation should be of general applicability since the distinctive features of the semifluidized bed as well as the hydrodynamic and drag features of the fluidized bed are accounted for.

To test the validity of Equation (5) several runs were carried out in the 1.54-in. diam. reactor described earlier. The limits of the different variables studied are given below.

Density of the particle	67.5 to 144.2 lb./cu.ft.
Diameter of the particle	0.0006 to 0.0018 ft.
Initial static bed height	About threefold variation
Overall height of the semifluidization column	About threefold variation

The principal features of the solids used are summarized in Table 1. About six hundred experimental determinations were made by changing the variables systematically within the limits mentioned above. The data were then programmed on a CDC 3600 computer and the constants of Equation (5) were determined. The resulting equation is

$$\frac{G_s}{G_t} = 2.15\, (Ar)^{-0.15}\, (Sf)^{-0.186} \qquad (6)$$

which represents all the experimental points with a standard deviation of 0.07051 and percentage deviation of 14.5. Only six experimental points showed deviations of the order of 50% while more than three hundred points showed deviations of less than 10%. Unlike the earlier correlations (*6, 10*), which were derived for a simple semifluidization column without a tubular section, Equation (6) holds regardless of the number and length of tubes in the tubular bundle, since it is based on the distribution of solids between the mixed and tubular portions. This was confirmed by carrying out several experiments with and without tubes and with varying number of tubes. It should be noted, however, that Equation (6) is restricted to particles of narrow size range, since the quantity of solids in the packed portion would obviously be greater in the presence of a larger proportion of fines.

The new group postulated, which may be termed the *semifluidization group*, is based on a characteristic length $(h - h_s)$ which is more important than either the static height or the overall height of the semifluidized bed. It may be noted that a third, very dilute, phase can sometimes be recognized between the packed and fluidized portions, and in the present analysis this has been treated as part of the fluidized bed. It was found experimentally that for a given overall height of the semifluidized bed, G_s decreases with the height of the static bed, that is, as $(h - h_s)$ increases the semifluidization velocity increases.

TABLE 1. PROPERTIES OF SOLIDS USED

Material	Particle density, lb./cu. ft.	Size range, ft.	Static bed porosity
Polystyrene beads	67.5	0.0006 to 0.0018	0.40 to 0.45
Sand	144.2	0.0006 to 0.0018	0.51 to 0.56
Glass beads	106.0	0.0006 to 0.0018	0.44 to 0.49
Bauxite	130.0	0.0006 to 0.0018	0.48 to 0.52
Silica gel	83.0	0.0006 to 0.0018	0.55 to 0.60

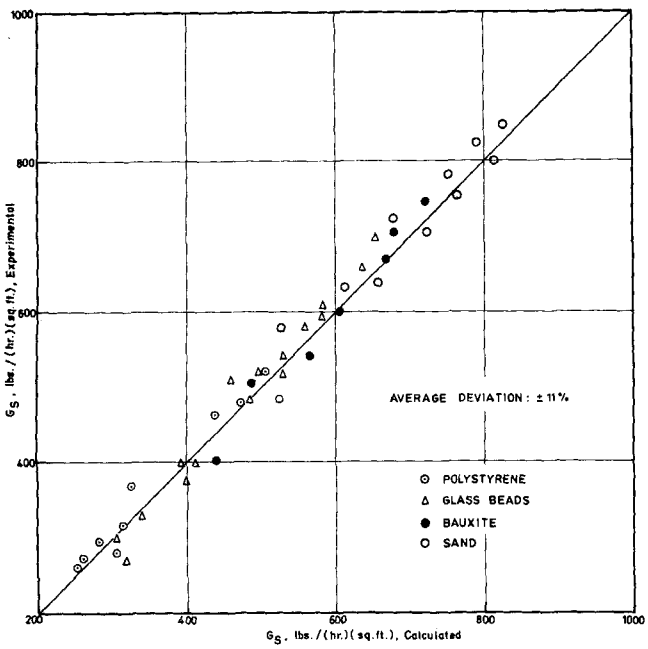

Fig. 4. Comparison of experimental and calculated minimum semifluidization velocities.

Preliminary analysis of the data clearly established a correlation between $(h - h_s)$ and G_s.

To generalize Equation (6) for semifluidized beds with different diameters, the constant 2.15 has to be suitably altered. For this purpose the term $(W_s - W_p)$ in the semifluidization number has to be expressed in terms of unit area. To maintain the dimensionless character of the semifluidization number, $(W_s - W_p)$ can be retained as such and the area term taken out and a new constant defined as

$$\frac{G_s}{G_t} = k\,(Ar)^{-0.15}\,(Sf)^{-0.186} \qquad (7)$$

where

$$k = \frac{17.3}{(D)^{-0.372}} \qquad (8)$$

(D is in feet).

To test the applicability of Equation (7), experiments were carried out in the 4-in. diam. reactor (2½ times the diameter of the first column) described earlier, and it was found that by using the constant calculated from Equation (8) the data could be correlated by Equation (7) to within about 15%. Thus Equation (7) can be considered as a general equation for predicting the performance of semifluidized MT reactors.

The onset of semifluidization (that is, the minimum semifluidization velocity) for several combinations of bed dimensions and particle properties was also determined by the usual ΔP vs. G curves, and it was found that Equation (7) represents the onset of semifluidization to within about 11%. Figure 4 shows a graphical comparison of the experimental and calculated minimum semifluidization velocities for a few randomly selected experimental points.

CONCLUSION

In this communication the earlier equation proposed for predicting the performance of semifluidized beds has been modified to give equations which predict the performance of MT semifluidized bed reactors with an average deviation of 14.5%. The same equations hold equally well for estimating the onset of semifluidization. It has been found that the assumption that the porosity of the packed bed is equal to that of the least static bed would lead to an error of the order of 15%. The proposed equations employ two dimensionless groups: the Archimedes group and a new group termed the *semifluidization group*. More work on a pilot-plant scale to test the validity of the proposed equations for reactors of very large diameters is required.

ACKNOWLEDGMENT

The authors wish to thank A. U. Momin, A. B. Mantri, and V. Nataraj for assistance in the course of this work.

NOTATION

Ar = Archimedes number, dimensionless group
d_p = geometric mean diameter of particle, ft.
D = diameter of reactor, ft.
E_f = void fraction in the fluidized bed
E_p = void fraction in the packed bed
E_s = void fraction in the static bed before fluidization
g_c = gravitational constant, ft./sec.^{2}
G = mass velocity, lb./(hr.)(sq.ft.)
G_f = fluidization velocity, lb./(hr.)(sq.ft.)
G_{mf} = minimum fluidization velocity, lb./(hr.)(sq.ft.)
G_{ms} = minimum semifluidization velocity, lb./(hr.)(sq. ft.)
G_s = semifluidized velocity, lb./(hr.)(sq.ft.)
G_t = terminal velocity, lb./(hr.)(sq.ft.)
h = overall height of the semifluidized bed, ft.
h_p = height of the top packed bed in semifluidized bed, ft.
h_s = height of the initial static bed, ft.
k = constant of dimensionless Equation (5)
MT = mixed tubular reactor system
ΔP = pressure drop, lb./sq.ft.
Sf = semifluidization group, dimensionless group
W_p = packed bed weight, lb.
W_s = initial weight of the static bed, lb.
ρ_F = density of the fluid, lb./cu.ft.
ρ_s = density of the solids, lb./cu.ft.
μ = viscosity of the fluid, lb./hr.ft.

LITERATURE CITED

1. Aris, Rutherford, *Can. J. Chem. Eng.*, **40**, 87 (1962).
2. Baker, P. I., and P. M. Beertjes, *Brit. Chem. Eng.*, **3**, 240 (1958).
3. Babu Rao, K., S. P. Mukherjee, and L. K. Doraiswamy, *A.I.Ch.E. J.*, **11**, 741 (1965).
4. Beranch, Y., and D. Sokol, *Khim. Prom.*, **1**, 62 (1959); *Chem. Abstr.*, **54**, 10419a (1960).
5. Bena, J., J. Ilavsky, and E. Kossaczky, *Chem. Prumysl*, **10**, 285 (1960); *Chem. Abstr.*, **54**, 20360b (1960).
6. Chin-Yung Wen, Wang Shih-Chung, and L. T. Fan, *A.I.Ch.E. J.*, **9**, 316 (1963).
7. Dotson, J. M., J. H. Holden, C. B. Seibert, H. P. Simons, and L. D. Schmidt, *Chem. Eng.*, **56**, No. 10, 128 (1949).
8. Dotson, J. M., *A.I.Ch.E. J.*, **5**, 169 (1959).
9. Douglas, J. M., *Chem. Eng. Progr. Symp. Ser. No. 48*, **61**, 1 (1964).
10. Fan, Liang-Tseng, and Chin-Yung Wen, *A.I.Ch.E. J.*, **7**, 4, 609 (1961).
11. Fan, Liang-Tseng, Yung-Chia Yang, and Chin-Yung Wen, *ibid.*, **5**, 407 (1959).
12. Gelperin, N. I., V. G. Ainstein, and I. D. Goikhman, *Intern. Chem. Eng. J.*, **5**, 55 (1965).
13. Grek, F. Z., and V. N. Kisel'nikov, *ibid.*, **4**, 263 (1964).
14. King, R. P., *Chem. Eng. Sci.*, **20**, 537 (1965).
15. Marsheck, R. M., and G. Albert, *ibid.*, **11**, 167 (1965).
16. Nangu Makato, *Z. Khim.*, **3**, 16 (1962).
17. Ranser, J. H., and J. W. Hickey, *Ind. Eng. Chem.*, **41**, 1244 (1949).
18. Reiss, T., *Bull. Assoc. Franc. Tech. Petrol*, **76**, 3 (1949).